Comparative study of GeO_2/Ge and SiO_2/Si structures on anomalous charging of oxide films upon water adsorption revealed by ambient-pressure X-ray photoelectron spectroscopy

Daichi Mori, Hiroshi Oka, Takuji Hosoi, Kentaro Kawai, Mizuho Morita, Ethan J. Crumlin, Zhi Liu, Heiji Watanabe, and Kenta Arima'

Citation: Journal of Applied Physics **120**, 095306 (2016); doi: 10.1063/1.4962202
View online: http://dx.doi.org/10.1063/1.4962202
View Table of Contents: http://aip.scitation.org/toc/jap/120/9
Published by the American Institute of Physics

Comparative study of GeO_2/Ge and SiO_2/Si structures on anomalous charging of oxide films upon water adsorption revealed by ambient-pressure X-ray photoelectron spectroscopy

Daichi Mori,[1] Hiroshi Oka,[2] Takuji Hosoi,[2] Kentaro Kawai,[1] Mizuho Morita,[1] Ethan J. Crumlin,[3] Zhi Liu,[3] Heiji Watanabe,[2] and Kenta Arima[1,a)]
[1]*Department of Precision Science and Technology, Graduate School of Engineering, Osaka University, 2-1, Yamada-oka, Suita, Osaka 565-0871, Japan*
[2]*Department of Material and Life Science, Graduate School of Engineering, Osaka University, 2-1, Yamada-oka, Suita, Osaka 565-0871, Japan*
[3]*Advanced Light Source, Lawrence Berkeley National Laboratory, Berkeley, California 94720, USA*

(Received 21 May 2016; accepted 22 August 2016; published online 2 September 2016)

The energy difference between the oxide and bulk peaks in X-ray photoelectron spectroscopy (XPS) spectra was investigated for both GeO_2/Ge and SiO_2/Si structures with thickness-controlled water films. This was achieved by obtaining XPS spectra at various values of relative humidity (RH) of up to ~15%. The increase in the energy shift is more significant for thermal GeO_2 on Ge than for thermal SiO_2 on Si above $\sim 10^{-4}$% RH, which is due to the larger amount of water molecules that infiltrate into the GeO_2 film to form hydroxyls. Analyzing the origins of this energy shift, we propose that the positive charging of a partially hydroxylated GeO_2 film, which is unrelated to X-ray irradiation, causes the larger energy shift for GeO_2/Ge than for SiO_2/Si. A possible microscopic mechanism of this intrinsic positive charging is the emission of electrons from adsorbed water species in the suboxide layer of the GeO_2 film to the Ge bulk, leaving immobile cations or positively charged states in the oxide. This may be related to the reported negative shift of flat band voltages in metal-oxide-semiconductor diodes with an air-exposed GeO_2 layer. *Published by AIP Publishing.*
[http://dx.doi.org/10.1063/1.4962202]

I. INTRODUCTION

The miniaturization of silicon (Si) metal-oxide-semiconductor field-effect transistors (MOSFETs) has been pursued in the last few decades with the aim of achieving both high performance and low power consumption. However, it is becoming increasingly challenging to scale down MOSFETs because of a variety of physical problems such as the short channel effect, gate leakage current, and parasitic resistance/capacitance. Because these problems lead to increased power consumption and the degradation of device performances, it is important to introduce a channel material with higher mobility than Si, which is expected to lead to higher device performances without relying on a conventional scaling scheme.

Germanium (Ge) is regarded as a promising channel material for future MOSFETs because of its higher holes and electron mobilities than those of Si.[1,2] Another advantage of Ge is its process compatibility with Si-based MOS technologies. Because of these advantages, various attempts have recently been made to fabricate Ge-based MOS devices. Although Ge oxide (GeO_2) is the most fundamental insulator in these devices, it decomposes at low temperatures[3,4] and is soluble in water,[5] unlike the more familiar Si oxide (SiO_2). In spite of these physical instabilities of the bulk, the GeO_2/Ge interface is still attractive because of its excellent electrical properties.[6] Researchers have developed a wide range of gate stack structures with a GeO_2/Ge interface. One approach is to use thermal or plasma techniques such as nitridation to passivate a GeO_2 surface by forming a GeON layer on top of GeO_2.[7] Another approach is to cap the GeO_2 surface by the deposition of high-k dielectric layers.[8,9] Metal-oxide-doped GeO_2 such as yttrium-GeO_2 has attracted interest because of its stronger resistance to liquid water than pure GeO_2.[10,11]

The above studies indicate that GeO_2 is a key material in Ge-based MOSFETs, and it is still necessary to grasp the relationship between the physical/chemical properties of GeO_2 and its dielectric properties. Among these properties, the effect of the microscopic interaction of water vapor on the quality of the GeO_2/Ge structure is a serious concern that should be clarified. Several groups have so far investigated this issue. Hosoi *et al.*[12] and Oniki *et al.*[13,14] reported the electrical characteristics of metal/GeO_2/Ge structures and revealed a negative shift of the flat-band voltage (V_{FB}) as well as anomalous hysteresis and a minority career response upon exposure to air. Diverse physical analyses such as by thermal desorption spectroscopy, infrared spectroscopy, and secondary ion mass spectrometry revealed the origin to be infiltration of adsorbed water or organic molecules into the GeO_2 film.[12–15]

X-ray photoelectron spectroscopy (XPS) is a powerful tool for identifying various properties of oxide/semiconductor structures. Analysis of the chemical shift of oxidation states is especially important for determining the oxide thickness, suboxide structure, and band offset. However, as Zhang *et al.*

a)Author to whom correspondence should be addressed. Electronic mail: arima@prec.eng.osaka-u.ac.jp

pointed out,[16] this fundamental issue is still controversial in the case of GeO_2 films on Ge. Recently, we conducted ambient-pressure XPS (AP-XPS) measurements on an annealed GeO_2 film on Ge in water vapor and demonstrated that the chemical shift of the GeO_2 peak (Ge^{4+}) from the bulk $3d_{5/2}$ increases with increasing relative humidity (RH) up to 1%.[17] In the present study, we obtained more AP-XPS spectra with synchrotron radiated light to investigate the chemical shift of GeO_2 on Ge in the presence of a thin water film in detail. By comparing the results with those for SiO_2/Si, we unveil the impact of the adsorption of water molecules on the quality of thin GeO_2 films on Ge.

II. EXPERIMENTAL DETAILS

A. Sample preparation

In most experiments, we used p-type Ge(100) and Si(100) wafers with resistivities in the range of 0.1–0.5 Ω cm and 0.1–6.0 Ω cm, respectively. Another n-type Si(100) wafer whose resistivity was less than 1Ω cm was also sometimes used. For the Ge samples, we formed sacrificial oxides by dry oxidation at 450 °C for 30 min in a conventional furnace and cleaned them by cyclic treatment using dilute HF (5%) and ultrapure water. Then, thin GeO_2 films were formed on the Ge substrate by dry oxidation at 550 °C. The Si samples were rinsed with ultrapure water, cleaned with a H_2SO_4/H_2O_2 solution, etched with a dilute HF solution (1%), and rinsed with ultrapure water. They were oxidized at 1000 °C in a cold-wall-type reaction chamber[18] in O_2 ambient. The GeO_2/Ge and SiO_2/Si samples were stored immediately in a vacuum desiccator evacuated by a diaphragm pump and were transferred to an AP-XPS chamber. All the Ge and Si samples were annealed at 300 °C for 30 min in a vacuum prior to the exposure to water vapor. This thermal treatment is referred to as preannealing hereafter.

B. AP-XPS experiments

AP-XPS measurements were performed at beamline 9.3.2 of the Advanced Light Source (ALS) of the Lawrence Berkeley National Laboratory. The X-ray flux was approximately 5×10^{10} photons/s.[19] A differentially pumped electrostatic lens system separated the AP-XPS chamber from a hemispherical photoelectron spectrometer, which enabled us to collect photoelectrons in gases at pressures of up to several Torr.[19–21] The energy resolution of the beamline is about $E/\Delta E = 3000$.[19] We used commercial water (Aristar Plus HPLC, low TOC grade) from The British Drug Houses (BDH) with a total organic carbon content of less than 20 ppb as the source of the water vapor. After the water was degassed in freeze-pump-thaw cycles, it was introduced into the XPS chamber under an ultrahigh vacuum (UHV) condition at a pressure of up to 1.0 Torr. In this article, we define UHV as pressures lower than 6×10^{-8} Torr. We also controlled the sample temperature using a chiller, with which the lowest temperature achieved was −9.6 °C. These procedures enabled us to obtain AP-XPS spectra in the humidity range of 0%–15%. The bulks of the Ge and Si samples were grounded.

Unless otherwise stated, the X-ray conditions were as follows. The spectra of the Ge 3d, Si 2p, O 1s, and C 1s core levels were obtained at incident photon energies of 350, 420, 855, and 610 eV, respectively. Because photoelectrons from these levels have similar kinetic energies of approximately 320 eV, we ensured that the probing depth was similar when obtaining the photoelectron spectra. The X-ray flux at 350 eV was similar to that at 420 eV. Ge 3d and Si 2p spectra were also collected at a photon energy of 855 eV. We obtained each spectrum by averaging at least three spectra to improve the signal-to-noise ratio; this took longer than 150 s. The pass energy was set to 100 eV. The binding energy scales of spectra taken on GeO_2/Ge and SiO_2/Si samples were calibrated using the known values for elemental Ge $3d_{5/2}$ (29.36 eV) and Si $2p_{3/2}$ (99.4 eV), respectively.[22–24] We used the NIST database to obtain the inelastic mean free path (IMEP) of electrons in Ge, Si, GeO_2, SiO_2, H_2O, and C.[25]

The oxide thicknesses of the thermal GeO_2 and SiO_2 films were in the ranges of 1.4–2.8 nm and 1.7–3.7 nm, respectively, which were estimated from the Ge 3d or Si 2p spectra using the formula proposed by Himpsel *et al.*[26] We found that this estimation has an error of ±0.20 nm due to statistical dispersion. Assuming 0.3 nm per carbon layer, the amount of carbon contamination was estimated to be 0.1–0.5 and 0.05–0.3 monolayers for GeO_2 and SiO_2 surfaces after preannealing, respectively. The contamination level on GeO_2 tended to be higher than that on SiO_2, probably because a GeO_2 film absorbs organic molecules unlike SiO_2.[15]

An O 1s spectrum together with a Ge 3d spectrum and a Si 2p spectrum were used to estimate the water layer thickness under an equilibrium condition on GeO_2 and SiO_2 surfaces, respectively. In the presence of water vapor, the O 1s spectrum after Shirley background subtraction included contributions from oxygen in the oxide film, in the adsorbed water species, and in the gas phase. Some examples of O 1s spectra are shown in Fig. 1. After the peaks were separated by peak fitting, the water layer thickness on the oxide surfaces was estimated from the separated peak areas. This was achieved by assuming a simple structure composed of three layers (water/oxide/semiconductor bulk). Details of this estimation are described elsewhere.[17,27] We found that the estimation of a peak area has a deviation of 5%. This leads to an error of about ±10% in the calculated water layer thicknesses. Noted that we cannot distinguish molecular water from surface hydroxyls because the energy difference between these two signals in O 1s spectra is too narrow for them to be separated.[17,28]

III. RESULTS AND DISCUSSION

Figure 2 shows XPS spectra obtained in UHV, whose investigation was the direct motivation of this study. Figure 2(a) was obtained after a GeO_2/Ge sample stored in a vacuum desiccator was exposed to ambient air and then introduced into an AP-XPS chamber. There are two main peaks: one is from the Ge bulk (Ge^{0+}) and the other is a chemical shift component from GeO_2 (Ge^{4+}). We analyzed the positions of the Ge $3d_{5/2}$ core line signals for the two components and found that the GeO_2(Ge^{4+}) Ge $3d_{5/2}$ component is

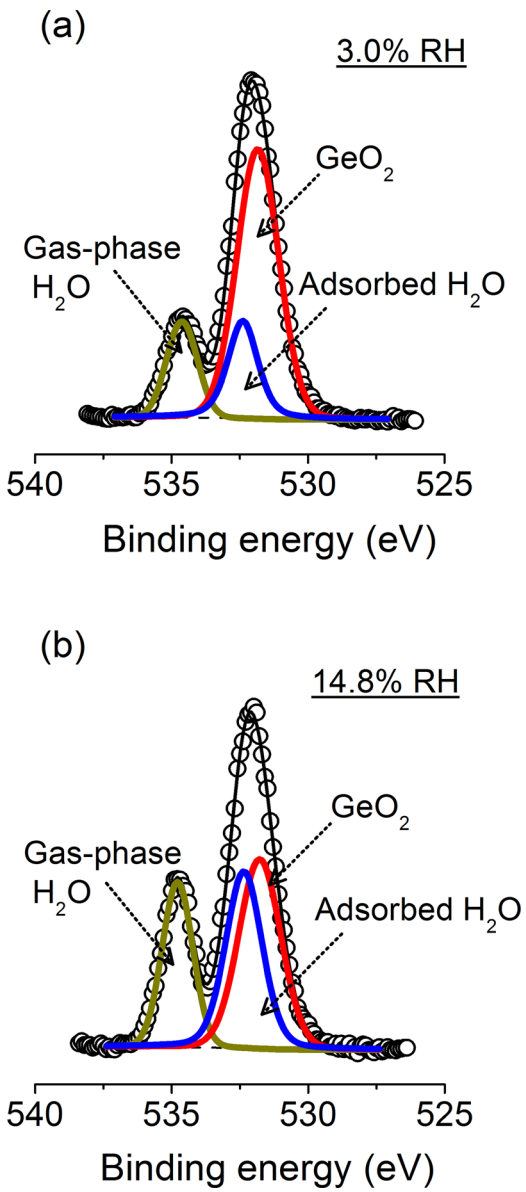

FIG. 1. Peak-fitted O 1s spectra on a GeO_2/Ge sample obtained at different values of RH. In each spectrum, the photoelectron intensity was normalized by the largest count. The area ratio of adsorbed water to the GeO_2 bulk in (b) is higher than that in (a), which indicates the formation of a thicker water layer in (b). See Ref. 17 for the procedure used to determine the peak areas of GeO_2 and adsorbed water in the O 1s spectra.

situated at 32.81 eV. This revealed that the energy difference between the two components is 3.45 eV in Fig. 2(a). We hereafter denote this energy difference, or the energy shift of the GeO_2 peak (Ge^{4+}) from the Ge bulk, as ΔE_{GeO_2}. Figure 2(b) shows the spectrum after preannealing of the sample in Fig. 2(a). We did not expose the annealed sample to ambient air but kept it and obtained the spectrum in UHV. The binding energy of the GeO_2(Ge^{4+}) Ge $3d_{5/2}$ component in Fig. 2(b) was found to be 32.47 eV, indicating that ΔE_{GeO_2} is 3.11 eV. This value is 0.34 eV smaller than that in Fig. 2(a), although the change in the oxide thickness (2.38 nm in Fig. 2(a) to 2.21 nm in Fig. 2(b)) is trivial. This decrease in the energy difference caused by the preannealing was not observed for SiO_2/Si. Namely, we conducted peak fitting of the measured spectra in Figs. 2(c) and 2(d) and analyzed the

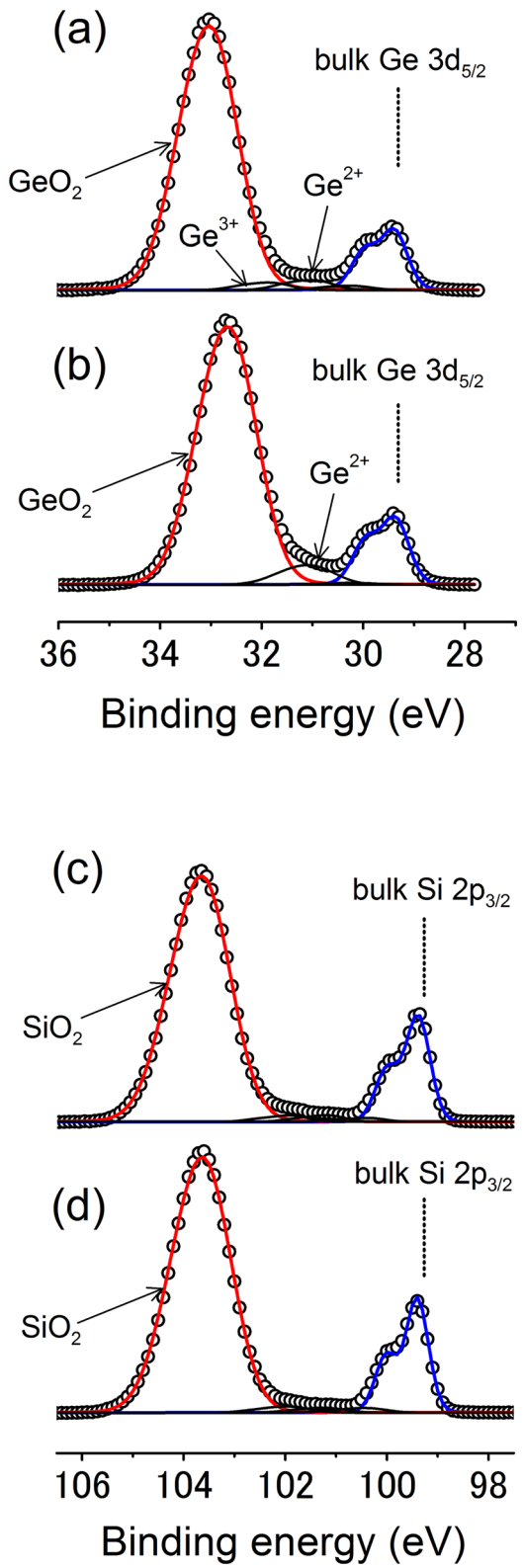

FIG. 2. Peak-fitted XPS spectra obtained in UHV. (a) Ge 3d spectrum of an air-exposed GeO_2/Ge sample. (b) Ge 3d spectrum after the sample in (a) was subsequently annealed at 300 °C for 30 min in a vacuum (preannealing). The shoulder peaks with binding energy close to 30 eV in (a) and (b) are both the Ge $3d_{3/2}$ lines from the Ge bulk. (c) Si 2p spectrum of an air-exposed SiO_2/Si sample. (d) Si 2p spectrum after preannealing of the sample in (c). The shoulder peaks with binding energy close to 100 eV in (c) and (d) are both the Si $2p_{1/2}$ lines from the Si bulk. The initial GeO_2 and SiO_2 thicknesses in (a) and (c) are 2.38 and 2.71 nm, respectively. The positions of the suboxide components (Ge^{1+}, Ge^{2+}, and Ge^{3+}) for the GeO_2/Ge sample are assigned from the literature,[29] whereas those for SiO_2/Si (Si^{+}, Si^{2+}, and Si^{3+}) were taken from another paper.[26]

positions of the Si $2p_{3/2}$ signals for both the oxide (Si^{4+}) and the substrate components. The SiO_2 (Si^{4+}) Si $2p_{3/2}$ components are situated at 103.51 and 103.48 eV in Figs. 2(c) and 2(d), respectively. Thus, we found that ΔE_{SiO_2} changes from 4.11 eV in Fig. 2(c) to 4.08 eV in Fig. 2(d), where ΔE_{SiO_2} represents the energy shift of the SiO_2 peak (Si^{4+}) from the Si bulk. The SiO_2 thicknesses in Figs. 2(c) and 2(d) were 2.71 and 2.67 nm, respectively. The thermal desorption spectra of molecules desorbed from the thermally grown GeO_2 and SiO_2 films indicated that GeO_2 has an unusual characteristic in terms of its absorbability of water molecules in air.[14,15] This strongly implies that the absorbance of moisture is the origin of the change in ΔE_{GeO_2} upon air exposure as shown in Figs. 2(a) and 2(b). It should be noted that the positions of the oxide and bulk peaks used to obtain ΔE_{GeO_2} and ΔE_{SiO_2} are influenced by the peak-fitting conditions such as the peak positions of the suboxides and the background subtraction. This results in errors in the calculated ΔE_{GeO_2} and ΔE_{SiO_2}. Unless otherwise stated, both ΔE_{GeO_2} and ΔE_{SiO_2} have an error of ± 0.04 eV.

Figure 3 shows water layer thicknesses as a function of relative humidity (RH). On the SiO_2 surface, the water coverage shows a rapid increase above 10^{-1}% and reaches 0.3 nm at 10%. This corresponds to approximately one layer (assuming 0.3 nm per water layer), which agrees with previous measurements by other groups.[28,30,31] On the other hand, thicker water films are formed on a GeO_2 surface than on SiO_2 at RH higher than 10^{-4}%, and one monolayer is achieved at a RH of approximately 1%. The thickness of the water layer rapidly increases above 1% RH, reaching 0.6–0.8 nm at 10% RH. Figure 3 demonstrates that a GeO_2 surface attracts a thicker water film than a SiO_2 surface in the RH range of 10^{-4}% to 10%. As mentioned in Section II, we cannot separate the component of surface hydroxyls from that of molecular water in O 1s spectra because their binding

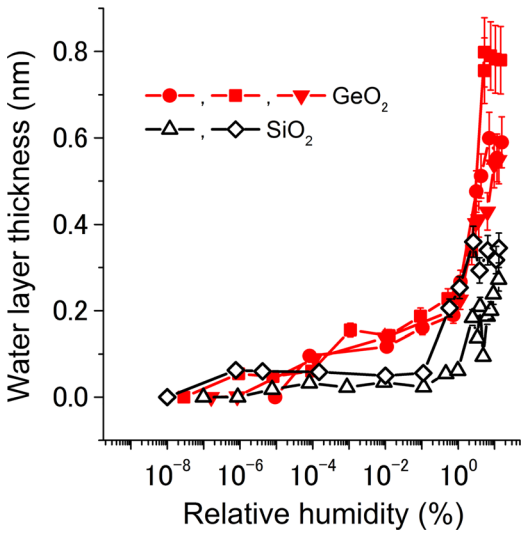

FIG. 3. Water layer thicknesses as a function of RH. Filled and open symbols represent data for GeO_2/Ge and SiO_2/Si, respectively. Symbols with different shapes indicate samples with different oxide thicknesses. Namely, the oxide thicknesses for the three GeO_2 samples were in the range between 1.8 nm and 2.8 nm, whereas those for the two SiO_2 samples were approximately 2.7 nm.

energies are too close. However, we speculate that the growth of the water layer on the GeO_2/Ge samples in the RH range between 10^{-4}% and around 1% in Fig. 3 mainly represents the hydroxylation of the GeO_2 film by the dissociative adsorption of water molecules. This is based on reports by other groups on the interaction of water vapor with the surfaces of various metal oxides including SiO_2.[28,32–35] In these studies, it was argued that the hydroxylation precedes the growth of a molecular water film, and the former starts at an RH of much lower than 1%. After the saturation of hydroxyl formation at a RH of around 1%, the adsorption of molecular water begins as a result of the attractive interaction between H_2O molecules and hydroxyls.[36] Considering the permeable nature of GeO_2, it seems reasonable to conclude from Fig. 3 that hydroxylation not only of the GeO_2 surface but also in the GeO_2 film starts at $\sim 10^{-4}$% RH. The sudden increase in the thickness above $\sim$1% RH in Fig. 3 indicates the formation of a molecular water film.

Next, we investigate the variation of both ΔE_{GeO_2} and ΔE_{SiO_2} with the thickness of the adsorbed water layer. This was achieved by obtaining the Ge 3d and Si 2p spectra at controlled values of RH on GeO_2 and SiO_2 surfaces, respectively. As shown in Fig. 4(a), ΔE_{GeO_2} and ΔE_{SiO_2} increase with RH for all GeO_2/Ge and SiO_2/Si samples. Moreover, we found that thicker oxide films tend to generate larger energy differences at a fixed RH. For example, ΔE_{GeO_2} at $\sim$1% RH is 3.67 and 3.47 eV on 2.73- and 1.85-nm-thick GeO_2 films, and ΔE_{SiO_2} is 4.44, 4.19, and 4.07 eV on 3.69-, 2.71-, and 1.76-nm-thick SiO_2 layers, respectively. These increases in ΔE_{GeO_2} and ΔE_{SiO_2} for thicker oxide films are known to occur in both the GeO_2/Ge and SiO_2/Si systems under a dry condition in UHV. In particular, for the latter system, its origin has been widely discussed on the basis of the final-state effect and charge trapping.[37–41]

We calculated the change in the energy difference ΔE_{GeO_2} or ΔE_{SiO_2} at an elevated RH from that at the lowest RH or in UHV for each sample, which is defined as ΔE_{change} hereafter. Namely, for both the GeO_2/Ge and SiO_2/Si samples

$$\Delta E_{change} = \Delta E_{elevated\,RH} - \Delta E_{UHV}, \quad (1)$$

in which $\Delta E_{elevated\,RH}$ and ΔE_{UHV} are ΔE_{GeO_2} (or ΔE_{SiO_2}) at a controlled RH in water vapor and that in UHV, respectively. Figure 4(b) shows ΔE_{change} obtained from the energy difference data in Fig. 4(a). Similar to ΔE_{GeO_2} or ΔE_{SiO_2}, as stated in an earlier paragraph, each plot of ΔE_{change} has an error of ± 0.04 eV. In Fig. 4(b), ΔE_{change} overlaps for the GeO_2 and SiO_2 surfaces up to 10^{-4}% RH. However, ΔE_{change} for the GeO_2/Ge samples increases more significantly than that for the SiO_2/Si ones at RH higher than 10^{-4}%. Also, the total increase in ΔE_{GeO_2} is 2–3 times larger than that in ΔE_{SiO_2} at 10% RH. As we pointed out for Fig. 3, 10^{-4}% is the critical RH around which the water layer starts to grow more rapidly on GeO_2 than on SiO_2. It seems reasonable to suppose that the more rapid increase in ΔE_{GeO_2} for GeO_2 above this critical RH in Fig. 4(b) is induced by the thicker water films than those on SiO_2.

Figure 5 shows the recovery properties of ΔE_{GeO_2} and ΔE_{SiO_2} when the water vapor in the AP-XPS chamber was

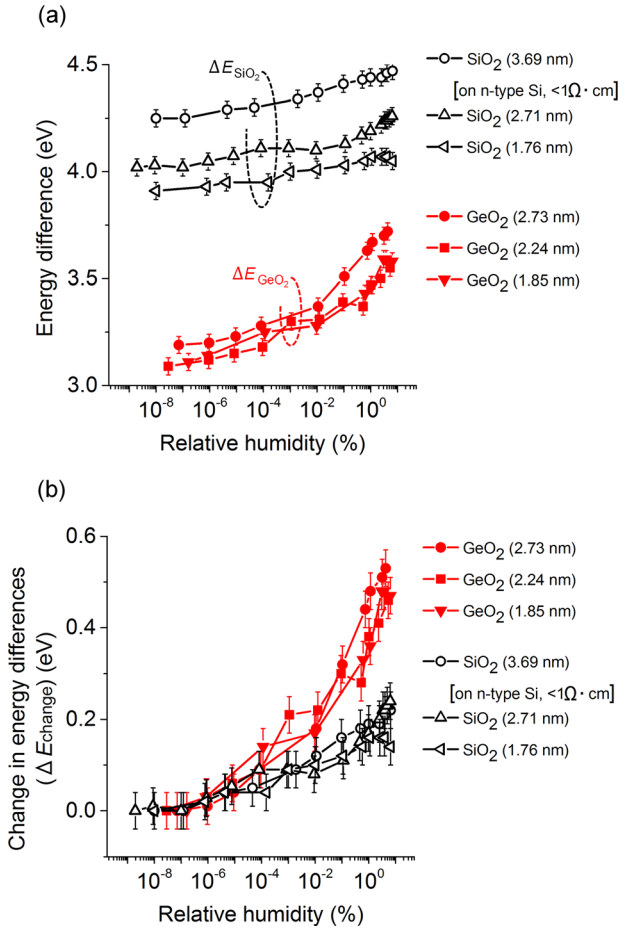

FIG. 4. (a) ΔE_{GeO_2} (filled symbols) and ΔE_{SiO_2} (open symbols) as a function of RH. Oxide thicknesses are indicated in parentheses in the legends. Most oxides were formed on p-type substrates except for the 3.69-nm-thick SiO_2 layer formed on an n-type substrate. (b) Changes in ΔE_{GeO_2} or ΔE_{SiO_2} at elevated RH from those taken in UHV, denoted as ΔE_{change}, for each sample in (a).

evacuated. Before 0 min, RH was set to ~5% on the sample surface by introducing water vapor (0.5 Torr). This resulted in an increase in both ΔE_{GeO_2} and ΔE_{SiO_2} compared with those in the initial vacuum, which is the reason for the positive values of ΔE_{change} at 0 min. The graph shows ΔE_{change} after evacuation by a turbomolecular pump starting at 0 min. For the SiO_2/Si samples, ΔE_{SiO_2} monotonically decreases after 0 min. After 100 min, it becomes less than 0.1 eV and approaches 0 eV. For the GeO_2/Ge samples, ΔE_{GeO_2} decreases after 0 min, similarly to that of the SiO_2/Si sample. However, it almost saturates at 0.3–0.4 eV after 200 min. This is probably due to water species remaining in the permeable GeO_2 films, as detected in our previous study.[17] This means that, in contrast to a SiO_2 surface, the exposure of a GeO_2 surface to water vapor appears to increase ΔE_{GeO_2} even if Ge 3d spectra are subsequently obtained in a vacuum of pressure lower than 1×10^{-6} Torr. Mild annealing at 300 °C is effective for returning ΔE_{GeO_2} and ΔE_{SiO_2} to close to their initial values obtained in UHV, as indicated by dashed lines in Fig. 5. These results in Fig. 5 are in agreement with those in Fig. 2.

Figures 2–5 imply that the formation of thin water films causes increases in both ΔE_{GeO_2} and ΔE_{SiO_2}. One possible reason is a change in the chemical bonds of the oxide

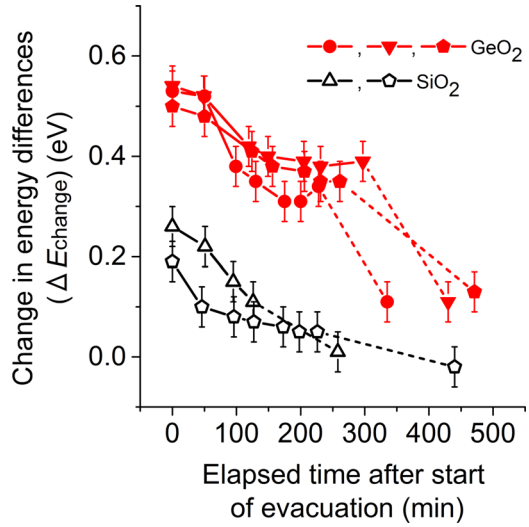

FIG. 5. Recovery properties of ΔE_{GeO_2} and ΔE_{SiO_2} as a function of elapsed time after the start of the evacuation of water vapor in the chamber. Dashed lines indicate how ΔE_{change} decreases upon annealing the samples at 300 °C for 10 min. Data plotted as pentagonal symbols were obtained from Ge 3d and Si 2p spectra with incident photon energies of 250 and 320 eV, respectively. These values ensure that photoelectrons had a similar kinetic energy of ~220 eV, whereas all other data were obtained using photoelectrons with a kinetic energy of ~320 eV.

network (i.e., the initial state change), but this can be ruled out because of the following results. Figure 6 shows the energy difference between the oxide (Ge^{4+}) and substrate Ge $3d_{5/2}$ peaks (ΔE_{GeO_2}) [plots in (a)], and that between the oxide in O 1s and Ge^{4+} in Ge $3d_{5/2}$ peaks (ΔE_{O-Ge}) [plots in (b)] as a function of RH. Ge 3d and O 1s spectra for the plots in Fig. 6 were collected at an incident photon energy of 855 eV. As shown in the insets, Ge 3d and O 1s spectra were peak-fitted, the procedures of which are the same as those in the cases of Figs. 2 and 1, respectively. In contrast to the rapid increase in ΔE_{GeO_2} at higher RH in Fig. 6(a), ΔE_{O-Ge} is nearly constant, as shown in Fig. 6(b). We conducted the same experiment as that in the case of Fig. 6 with Si 2p and O 1s spectra, and a trend similar to that in Fig. 6 was confirmed. These results indicate that the larger ΔE_{GeO_2} and ΔE_{SiO_2} at higher RH do not represent a change in the initial bonding states.

A straightforward explanation of the increases in ΔE_{GeO_2} and ΔE_{SiO_2} with thin water films is positive charging of the oxide films. We discuss its origin from the viewpoint of X-ray irradiation. Figure 7 shows the result of the time-lapse measurement of ΔE_{SiO_2} upon the X-ray irradiation of SiO_2/Si samples. The data in Figs. 7(a) and 7(b) were obtained in UHV and at 2.3% RH, respectively. Fig. 8 shows the expected band diagrams of the SiO_2/Si structures. In both graphs in Fig. 7, 0 min indicates the start of X-ray irradiation on an area of the surface that had not been exposed to X-rays. In Fig. 7(a), the initial ΔE_{SiO_2} is 3.95 eV. The schematic band diagram to exhibit this initial ΔE_{SiO_2} is assumed as Fig. 8(a). ΔE_{SiO_2} in Fig. 7(a) gradually increases to approximately 4.1 eV at 200 s, after which remains almost constant until 700 s. This increase in ΔE_{SiO_2} is due to the insulating SiO_2 film being positively charged by the emission of photoelectrons by X-ray irradiation. In other words, the

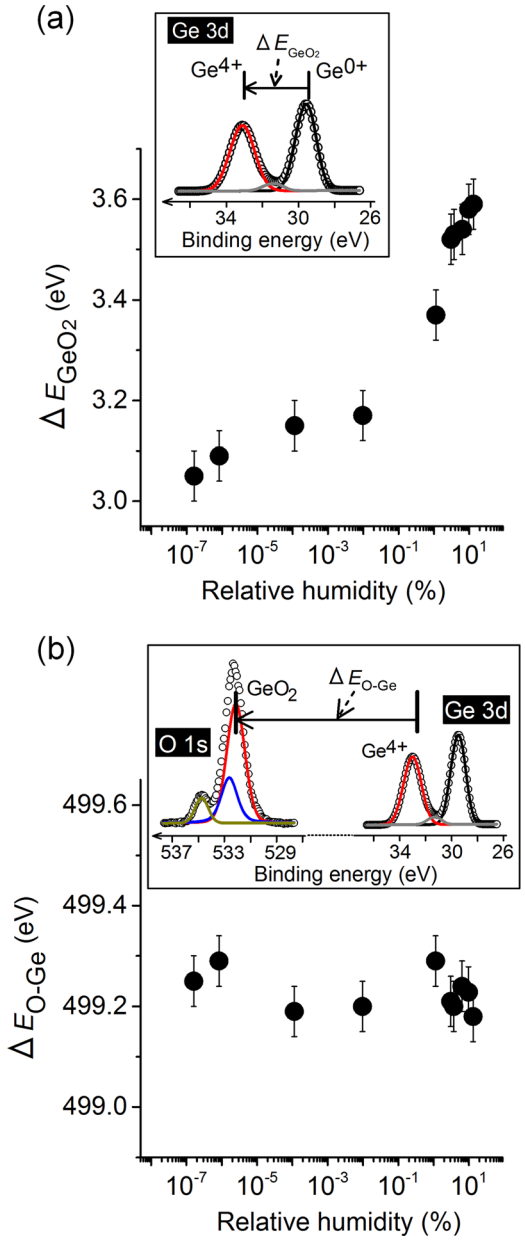

FIG. 6. (a) Energy differences as a function of RH (a) between the oxide (Ge^{4+}) and substrate Ge $3d_{5/2}$ peaks in Ge 3d spectra (ΔE_{GeO_2}) and (b) between the oxide in O 1s and oxide (Ge^{4+}) Ge $3d_{5/2}$ peaks (ΔE_{O-Ge}). In the O 1s spectrum in the inset in (b), red, blue and, ocher curves represent GeO_2, adsorbed H_2O including hydroxyls and gas-phase H_2O, respectively. Both O 1s and Ge 3d spectra were taken at the same photon energy of 855 eV. The GeO_2 thickness was 1.85 nm. Each data plot in (a) and (b) has an error of ±0.05 eV.

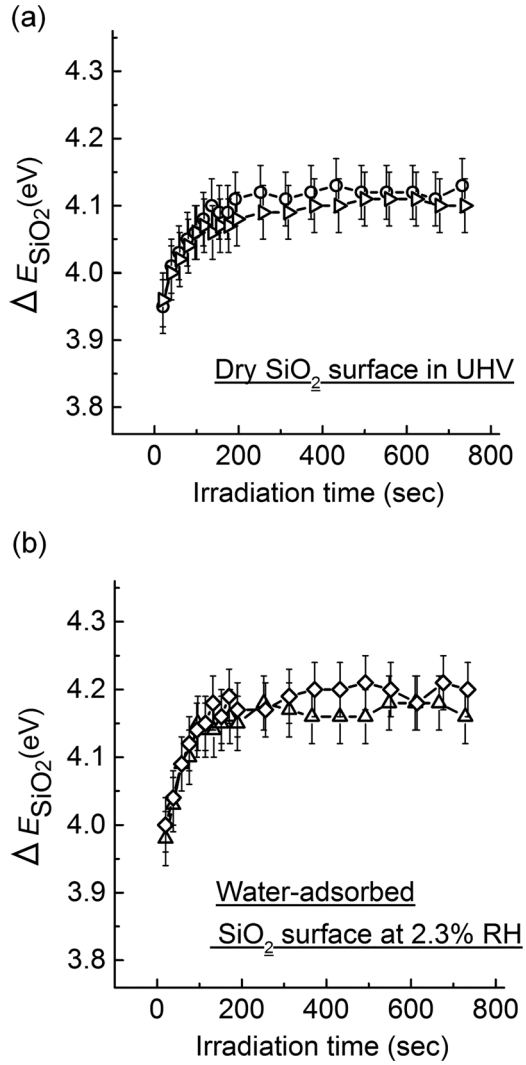

FIG. 7. ΔE_{SiO_2} as a function of elapsed time after the start of X-ray irradiation. (a) and (b) show the results obtained in UHV and in water vapor, respectively. The plots with different symbols were obtained on different areas of the surface of a SiO_2/Si sample with an oxide thickness of 2.36 nm that had not been exposed to X-rays. Each plot was obtained from a single Si 2p spectrum, rather than an averaged spectrum obtained from multiple raw spectra. Although this reduced the signal-to-noise ratio of the spectrum, it enabled us to rapidly obtain a spectrum in 18–20 s.

loss of electrons in the SiO_2 layer is not completely compensated only by tunneling electrons from the Si substrate. This creates a downward potential drop of ΔV_{ox} across the oxide layer, whose band diagram is schematically shown in Fig. 8(b).[40] This ΔV_{ox} is the origin of the increase in ΔE_{SiO_2} by prolonged X-ray irradiation of the structure in Fig. 7(a). In Fig. 7(b), ΔE_{SiO_2} increases rapidly by approximately 0.15 eV up to 200 s and then saturates. The net change in ΔE_{SiO_2} upon the prolonged irradiation of X-rays shown in Fig. 7(b) is 0.05–0.07 eV larger than that in Fig. 7(a). On the basis of the result in Fig. 3, the SiO_2 surface in Fig. 7(b) was probably covered by a one-monolayer water film. Because of the interaction of this thin water film, or adsorbed water species, with the X-ray beam, positive charging is enhanced compared with that for a dry SiO_2 surface (Fig. 7(a)). The expected band diagram in the case of both X-ray irradiation and water vapor is drawn in Fig. 8(c). The enhanced ΔV_{ox} explains why ΔE_{SiO_2} increases greatly on water-adsorbed SiO_2 under X-ray irradiation as shown in Fig. 7. Next, we used GeO_2/Ge samples to conduct similar experiments to those in Fig. 7, the results of which are shown in Fig. 9. We assume Fig. 10(a) to be the initial band diagram for a dry GeO_2 surface on Ge after preannealing. As shown in Fig. 9(a), ΔE_{GeO_2} increases again by approximately 0.1 eV in 300 s after the start of X-ray irradiation of a dry GeO_2 surface. This increase is due to the positive charging of the GeO_2 surface by X-ray irradiation or a downward potential drop of ΔV_{ox} across the oxide layer, whose band diagram is schematically shown in Fig. 10(b). In Fig. 9(b), ΔE_{GeO_2}

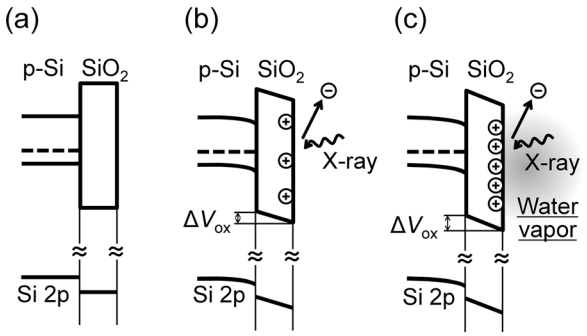

FIG. 8. Band diagrams for the SiO_2/Si structure. (a) and (b) Diagrams in UHV without and with X-ray irradiation, respectively. (c) With X-ray irradiation in water vapor.

increases monotonically during X-ray irradiation, and its increase reaches 0.15–0.2 eV after 700 s. This X-ray-induced positive charging appears to be more significant by 0.05–0.10 eV on a water-adsorbed GeO_2 surface than on a dry GeO_2 surface; this difference is similar to that for the SiO_2/Si samples shown in Fig. 7. What is striking is that the initial ΔE_{GeO_2} appears to be about 0.2 eV larger in Fig. 9(b) than in Fig. 9(a). This is contrary to the result for the SiO_2/Si samples in Fig. 7, in which the initial ΔE_{SiO_2} does not change significantly in the presence of a thin water film. This is likely to be unrelated to the X-ray irradiation, i.e., a *non*-X-ray effect, where the GeO_2 film is positively charged spontaneously by the adsorption of water molecules.

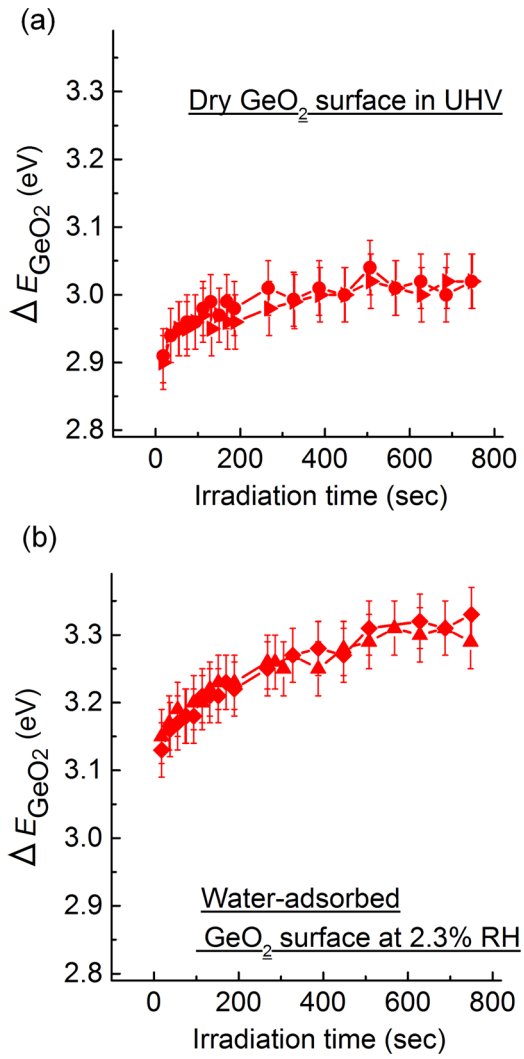

FIG. 9. ΔE_{GeO_2} as a function of elapsed time after the start of X-ray irradiation. The oxide thickness of the GeO_2/Ge sample was estimated to be 1.39 nm. The plots with different symbols were obtained on different areas of the surface that had not been exposed to X-rays. As mentioned in Fig. 7, each plot was obtained from a single Ge 3d spectrum to rapidly obtain a spectrum in 18–20 s.

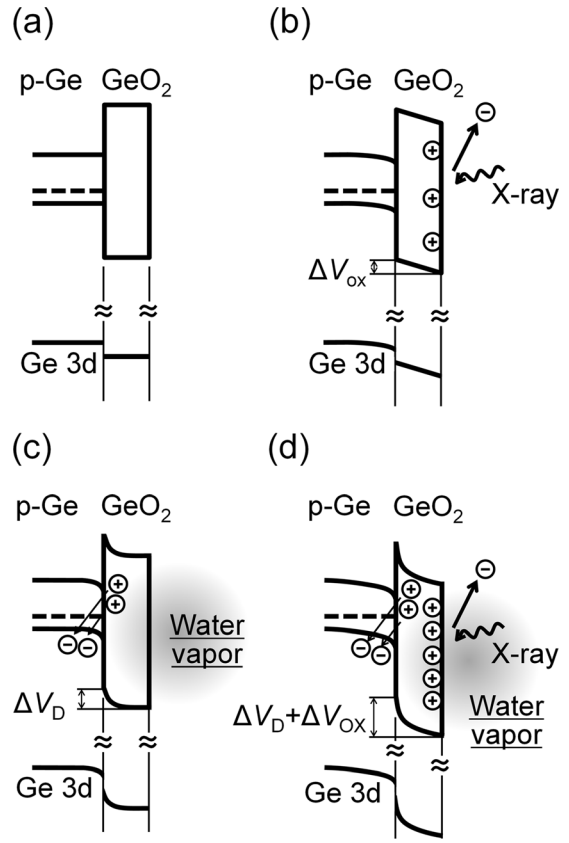

FIG. 10. Band diagrams for the GeO_2/Ge structure. (a) and (b) Diagrams in UHV without and with X-ray irradiation, respectively. (c) and (d) Diagrams on water-adsorbed GeO_2/Ge without and with X-ray irradiation, respectively.

To investigate the validity of this idea, we conducted another time-lapse measurement. Figure 11 shows the results, in which all the Si 2p and Ge 3d spectra were recorded with the same photon energy of 855 eV. The plots in Fig. 11 fluctuate because the photon flux of the X-rays used was lower than half of those in Figs. 7 and 9, which made it difficult to accurately conduct a peak-fitting analysis of the Si 2p or Ge 3d spectra. One important point in Fig. 11 is that the X-ray effect, i.e., the increase in the energy difference from the first plot to the last plot at approximately 800 s, appears to be less than those in Figs. 7 and 9, which is likely due to the smaller flux of X-rays in Fig. 11. We speculate from this result that the amount of positive charging of the oxide during X-ray irradiation depends on the X-ray conditions such as intensity and photon energy. Even more importantly, in the case of GeO_2/Ge, there is a marked increase in ΔE_{GeO_2} of approximately 0.2 eV between the first plots in Figs. 11(c) and 11(d). On the other hand, this *non*-X ray effect is absent in the SiO_2/Si system in Figs. 11(a) and 11(b).

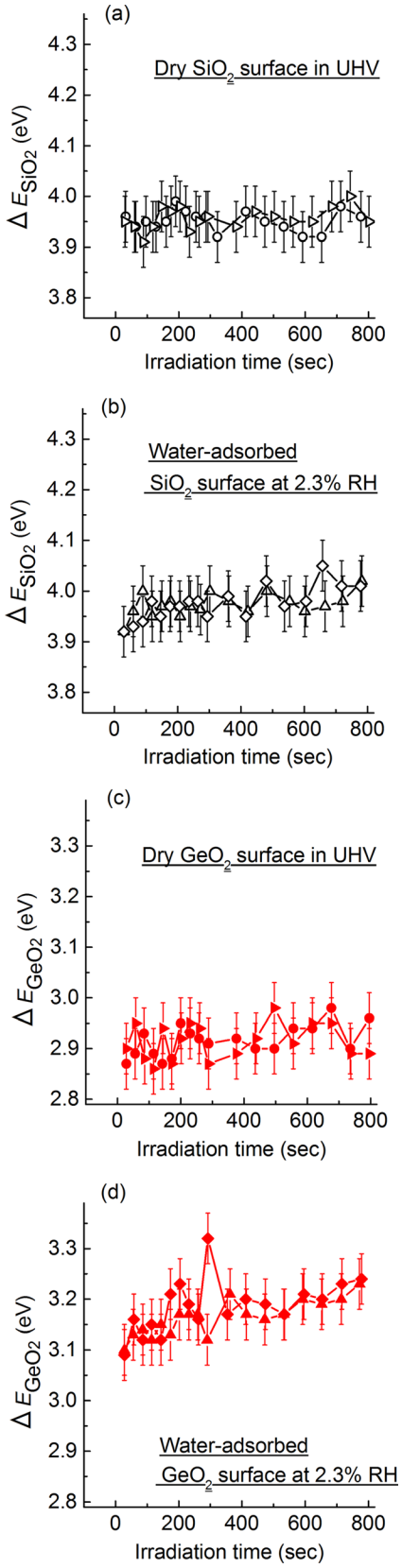

FIG. 11. (a) and (b) ΔE_{SiO_2} as a function of elapsed time after the start of X-ray irradiation of a 1.73-nm-thick SiO_2 film on Si. (c) and (d) ΔE_{GeO_2} as a function of elapsed time after the start of X-ray irradiation of a 1.51-nm-thick-GeO_2 film on Ge. The plots with different symbols were obtained on different areas of the SiO_2 or GeO_2 surface that had not been exposed to X-rays. All the raw Si 2p and Ge 3d spectra in (a)–(d) were obtained with the same incident photon energy (855 eV). It took 28–30 s to obtain each spectrum. Each data plot in (a)–(d) has an error of ±0.05 eV.

The results in Fig. 11 support our interpretation of the results in Fig. 9(b), in which the formation of a thin water film is considered to cause positive charging of a GeO_2 film that is unrelated to the X-ray irradiation. It took about 20 and 30 s to obtain the first plots in Figs. 9(b) and 11(d), respectively, after the start of X-ray irradiation. If some positive charges in GeO_2 films were built up by X-rays in a much shorter time scale, we would not be able to detect them as an X-ray-induced effect. However, the initial difference in ΔE_{GeO_2} between the first plots in Figs. 11(c) and 11(d) is similar to that in Figs. 9(a) and 9(b) in spite of the reduced flux of the X-rays, as mentioned in the previous paragraph. For this reason, although there is room for further investigation, we discuss the origin of the higher ΔE_{GeO_2} on the water-adsorbed GeO_2 film from the viewpoint of a *non*-X-ray effect.

Considering the permeability of GeO_2, a likely explanation is that electrons are transferred from the water-related species in GeO_2 to the Ge bulk upon exposure to water vapor, which causes positive charging of the films. A pioneering work in the 1970s showed that water molecules impacting on the surface of a GeO_2 film are instantaneously adsorbed and slowly diffuse deep into the film. This diffusion is paralleled by the fixation of H_2O on chemisorption sites in the film, accompanied by the ionization of H_2O molecules, causing them to emit electrons in the Ge bulk.[42] More recently, the generation of positive charges in GeO_2 films after exposure to air has been confirmed by a negative shift of V_{FB} in the capacitance-voltage (C-V) characteristics of metal/GeO_2/Ge diodes.[12–14] Because the C-V characteristics can be used to sense electrical properties, especially at an oxide/semiconductor interface, these results indicate that water molecules in air infiltrate the GeO_2 film, reaching the GeO_2/Ge interface, where they create positive charges. These reports agree with our data in Figs. 9(b) and 11(d), which show the spontaneous positive charging of the GeO_2 film by water adsorption.

In Fig. 4, in contrast to ΔE_{SiO_2}, ΔE_{GeO_2} begins to increase rapidly at a very low humidity of 10^{-4}%. As we reported previously, the increase in ΔE_{GeO_2} saturates above about 10% RH.[17] This means that this rapid increase in ΔE_{GeO_2}, or the generation of positive charges discussed above, is related to a structural change in the GeO_2 film that occurs in this low-RH range. A plausible explanation for this change is the partial hydroxylation of the film. As mentioned in the discussion of Fig. 3, we speculate that hydroxylation of the GeO_2 film occurred in the RH range between $\sim 10^{-4}$ and 1%. Then, what is the microscopic mechanism that creates positive charges in a partially hydroxylated GeO_2 film up to 1% RH? We previously reported the dependence of the suboxide structures of GeO_2/Ge samples on RH.[17] Although the peak areas of suboxides (Ge^{1+}, Ge^{2+}, Ge^{3+}) in Ge 3d spectra changed only slightly with the RH, we found that the peak area of Ge^{2+} tended to decrease gradually at an elevated RH up to ~1%, whereas that of Ge^{3+} increased monotonically. One example is shown in Fig. 2, in which the peak area of Ge^{2+} after preannealing in Fig. 2(b) is larger than that after air exposure with water vapor in Fig. 2(a). It was deduced that the initial abrupt GeO_2/Ge interface that existed after annealing in UHV collapsed upon hydroxylation at a

low RH of up to ~1% RH. This agrees with the result of a dynamic SIMS analysis of an air-exposed GeO_2/Ge sample, in which a certain amount of hydrogen was detected near the GeO_2/Ge interface.[15] It is likely that infiltrated water molecules promote hydroxylation to generate hole-trap states in the GeO_2 films, especially near the GeO_2/Ge interface or in the suboxide layer. These traps above the Ge Fermi level in the suboxide layer are positively charged by the electrons emitted to the Ge bulk, as suggested by Oniki and Ueno.[13] These positively charged states, or immobile cations, may be the origin of the *non*-X-ray-induced positive charging suggested by our XPS results in Figs. 9 and 11. Figures 10(c) and 10(d) depict the band diagrams of the water-adsorbed GeO_2/Ge system without and with X-ray irradiation, respectively. Unlike SiO_2/Si, a downward potential drop, or ΔV_D in Fig. 10(c), occurs spontaneously in a water-adsorbed GeO_2 film near the GeO_2/Ge interface. Because X-ray irradiation induces an additional potential drop (ΔV_{ox}), the total change in the potential ($\Delta V_D + \Delta V_{ox}$) becomes rather large upon X-ray irradiation in water vapor, as shown in Fig. 10(d). This large potential drop across the GeO_2 layer ($\Delta V_D + \Delta V_{ox}$) explains the significant increase in ΔE_{GeO_2} on a water-adsorbed GeO_2/Ge structure under X-ray irradiation in Figs. 9 and 11.

It is worth noting that the quality of a GeO_2 film can affect the amount of spontaneous positive charging of the GeO_2 film by water adsorption. It is widely accepted that the reaction at the GeO_2/Ge interface induced by heat treatment can cause GeO volatilization as follows:[3]

$$GeO_2(s) + Ge(s) \rightarrow 2GeO(g). \quad (2)$$

This GeO volatilization is known to occur even during a thermal oxidation process.[43] As discussed above with Fig. 10(c), infiltrated water molecules cause hydroxylation to generate hole-trap states in the suboxide layer of GeO_2 films. Thus, the hole-trap density is likely to depend on the thickness of the suboxide layer, which is determined by the GeO volatilization during the oxide growth. It is also imagined that the amount of infiltrated water molecules in the GeO_2 film itself is influenced by the suboxide layer thickness. Low-temperature oxidation, such as at 400 °C, is reported to be effective for reducing the suboxide layer thickness due to the suppression of GeO volatilization.[14] In our experiments, the oxidation temperature used to form GeO_2 films was set to 550 °C. If a GeO_2 film is formed at a lower temperature such as 400 °C, the suboxide layer will be thinner, leading to a lower hole-trap density. In such a case, the increase of ΔE_{GeO_2} due to the adsorption of water molecules, which was about 0.2 eV in Figs. 11(c) and 11(d), may be suppressed.

In Figs. 9(a) and 11(c), the initial ΔE_{Ge} on the newly annealed GeO_2 film is plotted as ~2.9 eV. This value is almost equal to the result for a thin Ge oxide film obtained by Matsui *et al.*[29] but much smaller than other values obtained by XPS such as 3.4 eV (Ref. 44) and 3.46 eV.[45] Then, what is the true chemical shift of a pure GeO_2 layer? One may think that the smaller value of ΔE_{GeO_2} is more accurate because water adsorption and X-ray-induced positive charging both increase ΔE_{GeO_2}. On the other hand, in the case of SiO_2/Si, many groups have reported the factors determining ΔE_{SiO_2}. In addition to charging and the change in chemical bonds, a final-state effect[37] is considered to be a key factor. This effect refers to a mechanism that stabilizes (or destabilizes) the core-hole state that is formed upon the ejection of a photoelectron from an emitting atom.[39] Namely, in a SiO_2/Si system, electrons ejected from the Si atoms in SiO_2 have a reduced binding energy due to the Coulomb interaction with the core holes because they are also subjected to the repulsion (screening) of their image charges in the Si bulk.[41] This effect is more significant in thinner SiO_2 films, and researchers have argued that the larger ΔE_{SiO_2} for a thicker SiO_2 layer of up to 2–3 nm thickness is mainly caused by this final-state effect.[39–41] Our small ΔE_{GeO_2} of ~2.9 eV in Figs. 9(a) and 11(c) may have been affected by the final-state effect because it was obtained with a GeO_2 film of thickness less than 2 nm. As demonstrated by another group[40] for the case of a SiO_2/Si system, the XPS spectra obtained on metal-coated GeO_2/Ge structures are expected to reveal more details on the actual chemical shift of the pure GeO_2 film.

The point of this study is that ΔE_{GeO_2} increases significantly when a GeO_2 film on a Ge bulk is partially hydroxylated. It is well known for SiO_2/Si that ΔE_{SiO_2} depends on the oxide thicknesses, and it is plausible that beam conditions such as the X-ray intensity and photon energy are also factors affecting ΔE_{SiO_2}. In addition to these parameters, water adsorption greatly affects ΔE_{GeO_2}. The amount of absorbed water molecules, or the extent of hydroxylation of the GeO_2 layer, depends on the sample preparation and the transfer method. For this reason, even in conventional XPS measurements in UHV, values of ΔE_{GeO_2} can be much more scattered than those of ΔE_{SiO_2} among different experiments and research groups. But if we carefully analyze the measured ΔE_{GeO_2}, it can be used to evaluate the quality of a thin Ge oxide.

IV. CONCLUSION

We conducted AP-XPS measurements of thin thermal GeO_2/Ge samples to investigate the relationship between the peak shift of an oxide (Ge^{4+}) from the bulk and the water layer thickness. This was achieved by using an AP-XPS setup to collect photoelectrons in water vapor up to a pressure of Torr order together with control of the sample temperature or RH on an oxide surface. We compared the results with those for thermally oxidized SiO_2 films on Si substrates. For similar beam intensities, we revealed that both ΔE_{GeO_2} and ΔE_{SiO_2} increase at an elevated RH of up to ~5% and that this trend is much clearer for ΔE_{GeO_2}. More specifically, the increase of ΔE_{change} for GeO_2/Ge is moderate up to ~10^{-4}% RH, which is similar to that for SiO_2/Si. After that, in contrast to ΔE_{SiO_2}, ΔE_{GeO_2} rapidly increases. Because the rapid growth of a water layer also starts above this critical RH (10^{-4}%), we expect that the increase in ΔE_{GeO_2} is caused by adsorbed water, rather than other species such as carbon-based contaminants. We find that ΔE_{GeO_2} remains larger than that of the initial annealed GeO_2/Ge sample once it is exposed to water vapor at ~5% RH, even if this vapor is

evacuated. This is more apparent for GeO_2/Ge than for SiO_2/Si, which indicates that ΔE_{GeO_2} depends on the amount of infiltrated water molecules in a GeO_2 layer. We also performed the time-lapse measurement of ΔE_{GeO_2} and ΔE_{SiO_2} after the start of X-ray irradiation on water-adsorbed oxide surfaces. It turned out that both SiO_2 and GeO_2 films are positively charged by X-ray irradiation and that this X-ray-induced positive charging is greater on water-adsorbed oxide surfaces than that on dry oxide surfaces. What was striking in this time-lapse measurement was that the initial ΔE_{GeO_2} for water-adsorbed GeO_2/Ge was ~0.2 eV higher than that of newly annealed GeO_2/Ge whereas no such difference was observed for SiO_2/Si. There are several possible explanations to account for this energy difference. One is beam-induced charging, in which the positive charging of a water-adsorbed GeO_2 film occurs most rapidly in the first 10–20 s after the start of irradiation. Another possibility is the intrinsic positive charging of a GeO_2 film upon water adsorption, which is caused by electron transfer from water species in the suboxide layer of a partially hydroxylated GeO_2 film to the Ge bulk. This intrinsic charging may be relevant to the negative shift of V_{FB} in MOS diodes with an air-exposed GeO_2 film. We obtained ΔE_{GeO_2} of ~2.9 eV on a 1.4-nm-thick GeO_2 film with neither adsorbed water molecules nor prolonged X-ray irradiation, which is smaller than the values in most reports. It follows from this study that special attention should be paid to the oxide peak in XPS spectra obtained from permeable oxide films.

ACKNOWLEDGMENTS

The authors wish to thank Dr. Hendrik Bluhm, Dr. Stephanus Axnanda, Sana Rani, Yusuke Saito, Yoshie Kawai, and Yuya Minoura for the operation of AP-XPS and valuable advice. This work was supported by the Japan Society for the Promotion of Science (JSPS) KAKENHI Grant Nos. JP24686020, JP26630026 and JP16K14133. This work was also supported in part by a grant from the Murata Science Foundation and the Mikiya Science and Technology Foundation. The Advanced Light Source is supported by the Director, Office of Science, Office of Basic Energy Sciences, of the U.S. Department of Energy under Contract No. DE-AC02-05CH11231.

[1]J. Robertson, Rep. Prog. Phys. **69**, 327 (2006).
[2]H. Shang, M. M. Frank, E. P. Gusev, J. O. Chu, S. W. Bedell, K. W. Guarini, and M. Ieong, IBM J. Res. Dev. **50**, 377 (2006).
[3]K. Kita, S. Suzuki, H. Nomura, T. Takahashi, T. Nishimura, and A. Toriumi, Jpn. J. Appl. Phys., Part 1 **47**, 2349 (2008).
[4]K. Kita, S. Suzuki, H. Nomura, T. Takahashi, T. Nishimura, and A. Toriumi, ECS Trans. **11**, 461 (2007).
[5]K. Prabhakaran and T. Ogino, Surf. Sci. **325**, 263 (1995).
[6]H. Matsubara, T. Sasada, M. Takenaka, and S. Takagi, Appl. Phys. Lett. **93**, 032104 (2008).
[7]K. Kutsuki, G. Okamoto, T. Hosoi, T. Shimura, and H. Watanabe, Appl. Phys. Lett. **95**, 022102 (2009).
[8]F. Bellenger, M. Houssa, A. Delabie, V. V. Afanas'ev, T. Conard, M. Caymax, M. Meuris, K. De Meyer, and M. M. Heyns, J. Electrochem. Soc. **155**, G33 (2008).
[9]A. Delabie, F. Bellenger, M. Houssa, T. Conard, S. Van Elshocht, M. Caymax, M. Heyns, and M. Meuris, Appl. Phys. Lett. **91**, 082904 (2007).
[10]C. M. Lu, C. H. Lee, W. F. Zhang, T. Nishimura, K. Nagashio, and A. Toriumi, Appl. Phys. Lett. **104**, 092909 (2014).
[11]C. Lu, C. H. Lee, W. Zhang, T. Nishimura, K. Nagashio, and A. Toriumi, J. Appl. Phys. **116**, 174103 (2014).
[12]T. Hosoi, K. Kutsuki, G. Okamoto, M. Saito, T. Shimura, and H. Watanabe, Appl. Phys. Lett. **94**, 202112 (2009).
[13]Y. Oniki and T. Ueno, Appl. Phys. Express **4**, 081101 (2011).
[14]Y. Oniki and T. Ueno, Jpn. J. Appl. Phys., Part 1 **51**, 04DA01 (2012).
[15]S. Ogawa, T. Suda, T. Yamamoto, K. Kutsuki, I. Hideshima, T. Hosoi, T. Shimura, and H. Watanabe, Appl. Phys. Lett. **99**, 142101 (2011).
[16]W. F. Zhang, T. Nishimula, K. Nagashio, K. Kita, and A. Toriumi, Appl. Phys. Lett. **102**, 102106 (2013).
[17]A. Mura, I. Hideshima, Z. Liu, T. Hosoi, H. Watanabe, and K. Arima, J. Phys. Chem. C **117**, 165 (2013).
[18]S. Morita, A. Shinozaki, Y. Morita, K. Nishimura, T. Okazaki, S. Urabe, and M. Morita, Jpn. J. Appl. Phys., Part 1 **43**, 7857 (2004).
[19]M. E. Grass, P. G. Karlsson, F. Aksoy, M. Lundqvist, B. Wannberg, B. S. Mun, Z. Hussain, and Z. Liu, Rev. Sci. Instrum. **81**, 053106 (2010).
[20]D. F. Ogletree, H. Bluhm, G. Lebedev, C. S. Fadley, Z. Hussain, and M. Salmeron, Rev. Sci. Instrum. **73**, 3872 (2002).
[21]M. Salmeron and R. Schlogl, Surf. Sci. Rep. **63**, 169 (2008).
[22]NIST X-ray Photoelectron Spectroscopy Database; National Institute of Standards and Technology: Gaithersburg, MD.
[23]C. J. Powell, J. Electron Spectrosc. Relat. Phenom. **185**, 1 (2012).
[24]Note that the bulk peak of Ge was fixed at 29.7 eV in our previous paper,[17] which was reported as the value for Ge 3d.[22] Because we found 29.36 eV to be the binding energy of a more specific Ge $3d_{5/2}$ core line signal for the Ge bulk,[23] we used it as the energy reference for the measured Ge 3d spectra.
[25]NIST Electron Inelastic-Mean-Free-Path Database; National Institute of Standards and Technology: Gaithersburg, MD.
[26]F. J. Himpsel, F. R. McFeely, A. Talebibrahimi, J. A. Yarmoff, and G. Hollinger, Phys. Rev. B **38**, 6084 (1988).
[27]K. Arima, P. Jiang, X. Y. Deng, H. Bluhm, and M. Salmeron, J. Phys. Chem. C **114**, 14900 (2010).
[28]A. Verdaguer, C. Weis, G. Oncins, G. Ketteler, H. Bluhm, and M. Salmeron, Langmuir **23**, 9699 (2007).
[29]M. Matsui, H. Murakami, T. Fujioka, A. Ohta, S. Higashi, and S. Miyazaki, Microelectron. Eng. **88**, 1549 (2011).
[30]D. B. Asay and S. H. Kim, J. Phys. Chem. B **109**, 16760 (2005).
[31]A. L. Sumner, E. J. Menke, Y. Dubowski, J. T. Newberg, R. M. Penner, J. C. Hemminger, L. M. Wingen, T. Brauers, and B. J. Finlayson-Pitts, Phys. Chem. Chem. Phys. **6**, 604 (2004).
[32]G. Ketteler, S. Yamamoto, H. Bluhm, K. Andersson, D. E. Starr, D. F. Ogletree, H. Ogasawara, A. Nilsson, and M. Salmeron, J. Phys. Chem. C **111**, 8278 (2007).
[33]X. Deng, T. Herranz, C. Weis, H. Bluhm, and M. Salmeron, J. Phys. Chem. C **112**, 9668 (2008).
[34]S. Yamamoto, T. Kendelewicz, J. T. Newberg, G. Ketteler, D. E. Starr, E. R. Mysak, K. J. Andersson, H. Ogasawara, H. Bluhm, M. Salmeron, G. E. Brown, and A. Nilsson, J. Phys. Chem. C **114**, 2256 (2010).
[35]J. T. Newberg, D. E. Starr, S. Yamamoto, S. Kaya, T. Kendelewicz, E. R. Mysak, S. Porsgaard, M. B. Salmeron, G. E. Brown, A. Nisson, and H. Bluhm, J. Phys. Chem. C **115**, 12864 (2011).
[36]S. Yamamoto, K. Andersson, H. Bluhm, G. Ketteler, D. E. Starr, T. Schiros, H. Ogasawara, L. G. M. Pettersson, M. Salmeron, and A. Nilsson, J. Phys. Chem. C **111**, 7848 (2007).
[37]G. Hollinger, Appl. Surf. Sci. **8**, 318 (1981).
[38]S. Iwata and A. Ishizaka, J. Appl. Phys. **79**, 6653 (1996).
[39]K. Z. Zhang, J. N. Greeley, M. M. B. Holl, and F. R. McFeely, J. Appl. Phys. **82**, 2298 (1997).
[40]H. Kobayashi, T. Kubota, H. Kawa, Y. Nakato, and M. Nishiyama, Appl. Phys. Lett. **73**, 933 (1998).
[41]J. W. Keister, J. E. Rowe, J. J. Kolodziej, H. Niimi, H. S. Tao, T. E. Madey, and G. Lucovsky, J. Vac. Sci. Technol. A **17**, 1250 (1999).
[42]E. K. Enikeev, A. Y. Loginov, and G. F. Golovanova, Russ. Chem. Bull. **24**, 2044 (1975).
[43]Y. Oniki, H. Koumo, Y. Iwazaki, and T. Ueno, J. Appl. Phys. **107**, 124113 (2010).
[44]D. Schmeisser, R. D. Schnell, A. Bogen, F. J. Himpsel, D. Rieger, G. Landgren, and J. F. Morar, Surf. Sci. **172**, 455 (1986).
[45]Y. Wang, Y. Z. Hu, and E. A. Irene, J. Vac. Sci. Technol. A **12**, 1309 (1994).